

Profile Shapes for Optically Thick X-ray Emission Lines from Stellar Winds

R. Ignace^{1,2} and K. G. Gayley²

ABSTRACT

We consider the consequences of appreciable line optical depth for the profile shape of X-ray emission lines formed in stellar winds. The hot gas is thought to arise in distributed wind shocks, and the line formation is predominantly via collisional excitation followed by radiative decay. Such lines are often modelled as optically thin, but the theory has difficulty matching resolved X-ray line profiles. We suggest that for strong lines of abundant metals, newly created photons may undergo resonance scattering, modifying the emergent profile. Using Sobolev theory in a spherically symmetric wind, we show that thick-line resonance scattering leads to emission profiles that still have blueshifted centroids like the thin lines, but which are considerably less asymmetric in appearance. We focus on winds in the constant-expansion domain, and derive an analytic form for the profile shape in the limit of large line and photoabsorptive optical depths. In this limit the emission profile reduces to a universal shape and has a centroid shift of $-0.24v_\infty$ with a HWHM of $0.63v_\infty$. Using published data for *Chandra* observations of five emission lines from the O star ζ Pup, we find that the observed HWHMs are somewhat smaller than predicted by our theory; however, the centroid shifts of all five lines are consistent with our theoretical result. These optical-depth effects can potentially explain the more nearly symmetric emission lines observed in ζ Ori, θ^1 Ori C, and δ Ori by *Chandra*, although an alternative explanation is required to account for the unshifted peak line emission. We also consider enhanced reabsorption by continuous opacity as line photons multiply scatter within an optically thick line, and find for lines with optical depths of a few that such reabsorption can further reduce the line asymmetry. It also reduces the line equivalent width, but probably not enough to alleviate the problem of sub-solar metallicities inferred from O star X-ray spectra by *ASCA*, unless the width of the resonance regions are superthermally enhanced.

Subject headings: Line: Profiles — Stars: Early-Type — Stars: Winds, Outflows — X-rays: Stars

¹ Email: ri@astro.physics.uiowa.edu

² 203 Van Allen Hall, Department of Physics and Astronomy, University of Iowa, Iowa City, IA 52242 USA

1. INTRODUCTION

Observations by the *Chandra* and *XMM-Newton* telescopes are providing first-ever resolved emission line profiles from early-type stellar winds in the X-ray band (the O star ζ Pup by Kahn et al. 2000 and Cassinelli et al. 2001; the O star θ^1 Ori C by Schulz et al. 2001; the O star ζ Ori by Waldron & Cassinelli 2001; and the O star δ Ori by Miller et al. 2001). Already, many early-type stars were known to be X-ray sources from observations by *EINSTEIN* and *ROSAT* (Harnden et al. 1979; Seward et al. 1979; Seward & Chlebowski 1982; Pollock 1987; Pollock, Haberl, & Corcoran 1995; Kudritzki et al. 1996; Berghöfer et al. 1997).

Although early attempts sought to explain the X-ray emission via stellar coronae (e.g., Cassinelli & Olson 1979; Waldron 1984), the currently favored model is based on considerations of stellar-wind shocks (e.g., Lucy & White 1980; Lucy 1982; Owocki, Castor, & Rybicki 1988; Feldmeier, Puls, & Pauldrach 1997). The highly successful line-driven wind theory for explaining hot star winds (Lucy & Solomon 1970; Castor, Abbott, & Klein 1975; Friend & Abbott 1986; Puls, Pauldrach, & Kudritzki 1986) is well suited to generating instabilities leading to shock structures distributed throughout the wind flow and giving rise to the production of hot gas.

The confrontation of theory with data has led to mixed results. For example, Feldmeier et al. (1997) conducted extensive modelling of wind shock X-ray production using time-dependent hydrodynamical simulations. Their sophisticated treatment includes a voluminous line list, but is limited to spherical symmetry, and only models for O stars have been investigated. Within this context, their efforts reveal that a single high-density shell will tend to dominate the observed X-ray emission. Such a feature should lead to significant variability which has not been observed (e.g., see Berghöfer & Schmitt 1995). Phenomenologically, perhaps their results apply in a “piecewise spherical” sense, whereby these X-ray bright events no longer occur in a single global shell, but as numerous smaller events occurring at different times. In this way, the variability can be suppressed (e.g., Oskinova et al. 2001).

Aside from the issues of global X-ray production and variability, the resolved emission line profiles in

four O stars (ζ Pup, ζ Ori, θ^1 Ori C, and δ Ori) appear to be truly problematic for the current theory. The X-ray emission is expected to be dominated by a spectrum of optically thin lines. In addition to the intervening ISM, the stellar wind itself can significantly contribute to the attenuation of shock generated X-rays. Consequently, the observed emission profiles are expected to be asymmetric, with peak line emission appearing blueshifted of line center, with the redshifted emission being more suppressed because there is a larger column depth of attenuation to the receding hemisphere of the wind (MacFarlane et al. 1991; Ignace 2001; Owocki & Cohen 2001). However, the observed line profiles for ζ Ori, θ^1 Ori C, and δ Ori appear to be quite symmetric. The emission lines for ζ Pup are far more consistent with the expectations of distributed wind shocks, but even for this star, the line morphologies may not be consistent with the current theory. So either the underlying wind model, or simply the assumptions used in deriving the emission-line profile shapes, must be modified. It is this latter case that is the focus of this work, with particular attention given to ζ Pup since it appears to best exemplify current standard wind-shock expectations.

Raymond & Smith (1977) made a major contribution to interpreting the X-ray emission from hot astrophysical plasmas by providing a cooling function that, among other processes, accounts for the emission by optically thin lines. Their results, along with better line data, have been used in the modelling efforts of numerous studies, including the topic at hand of stellar winds. However, some have questioned the assumption of effectively thin emission among the stronger wind lines in the X-ray band (e.g., Hillier et al. 1993; Kitamoto & Mukai 1996; Kitamoto et al. 2000). As will be discussed in §2, we find that it is possible for some lines to be optically thick. In §3, the formation of optically thick line profiles in distributed X-ray emitting zones for a stellar wind is considered using standard Sobolev theory. In particular, focus is given to the case of constant spherical expansion appropriate for relatively dense winds in which the X-ray emission escapes only from several radii out in the flow. This case is germane to the O stars which have been observed with *Chandra* and *XMM*. Optically thick emission not only alters the profile diagnostics, it presents the possibility for X-ray photon destruction,

which would invalidate the Raymond & Smith assumption for those lines. In §4, we consider the role of photon absorption in X-ray bound-free continua *within* the resonance zones in which the photons are created. A discussion of our results in relation to published observations is given in §5.

2. THE OPTICAL DEPTH OF X-RAY LINES

Should one expect wind emission lines produced in the X-ray band to be optically thick? As already stated, the primary process by which X-ray line photons are created is collisional excitation followed by radiative decay. For minority species, radiative recombination into excited states may also contribute, but for our purposes this may be viewed as essentially a collisional process as well. The key assumption is that the photon creation rate per volume scales with the square of the density. To estimate the optical depth, we consider a slab of X-ray emitting shocked gas. For a slab of initial temperature T_X , constant electron number density n_e , and volume cooling rate $\Lambda(T_X)$, the cooling time will be given roughly by

$$t_c \approx \frac{5}{2} \frac{k \Delta T}{n_e \Lambda(T_X)}. \quad (1)$$

The ΔT is to represent the range of temperatures over which a particular ion state i of some atomic species j exists in the slab for the purpose of estimating the line optical depth. The expression thus describes the cooling time for a particular ion species from $T_X + 0.5\Delta T$ to $T_X - 0.5\Delta T$.

The line optical depth is given roughly as

$$\tau \approx n_1 \sigma_l l_c \Delta\nu^{-1}, \quad (2)$$

where n_1 is the population number density of the ground state for the transition of interest, σ_l is the line integrated optical depth as given by

$$\sigma_l \approx \frac{\pi e^2}{m_e c} f_{12}, \quad (3)$$

which applies for a two-level atom that is strongly NLTE, l_c is the cooling length as given by

$$l_c = V t_c, \quad (4)$$

for V the speed of the postshock material, and $\Delta\nu = v_D/\lambda$ is the frequency width of the line opacity for Doppler broadening v_D and line wavelength λ .

For simplicity the Doppler broadening is just taken as the thermal speed of the hot gas, although turbulent motions could be important and somewhat larger. For NLTE, the population number density of the ground state is roughly equal to the entire number density for that ion n_i . Taking this to be the case, n_i can be re-expressed in terms of the ionization fraction q_i of the ion to all ions of the species and the relative abundance \mathcal{A}_j of the species to all nuclei n_N , giving $n_i \approx q_i \mathcal{A}_j n_N$. Thus the optical depth of the line formed in just this one slab becomes

$$\tau \approx \frac{5 k \Delta T q_i \mathcal{A}_j n_N \sigma_l \lambda V}{2 n_e \Lambda(T_X) v_{\text{th}}}. \quad (5)$$

We estimate the optical depth for O VIII Ly α at 19.0 Å as an example of a strong line in a gas with a solar composition of oxygen ($\mathcal{A}_j = 9 \times 10^{-4}$). From Sutherland & Dopita (1993), the ionization fraction of O VIII peaks at around 2 million K with a value of $q_i \approx 0.5$, which predominantly exists over a temperature range of $\Delta T \approx 2$ million K. The volume cooling rate is about 6×10^{-23} erg s $^{-1}$ cm 3 . The necessary shock jump is 500 km s $^{-1}$, and the thermal speed for hot oxygen is 45 km s $^{-1}$. Hence the optical depth for this one slab becomes $\tau \approx 10^2$. This demonstrates that it is entirely reasonable that the strong lines of metals with $\mathcal{A}_j \gtrsim 10^{-4}$, which includes many of the lines observed in hot star X-ray spectra, could be optically thick.

Having shown that optical thickness may be relevant for strong resonance lines, what should we expect for its influence on the emission profile shape? The observed profiles for ζ Pup (Kahn et al. 2001; Cassinelli et al. 2001) are asymmetric with blueshifted peak emission. As will be discussed further at a later point, photoabsorption by the ambient wind component generally accounts for this asymmetry. However, the effect of line optical depth is to alter the primary direction of photon escape. For example, the emissivity for a line that is thin is isotropic, and so there is no preferred escape

direction for photons. For a radially narrow but optically thick slab as considered above, photons escape primarily normal to the slab face, since the optical depth in that direction is least. For a large number of slabs at a fixed radius and uniformly distributed in solid angle, and ignoring the wind photoabsorption, those slabs that are fore and aft will tend to be the brightest based on this argument. Now accounting for the asymmetric photoabsorption across the line frequencies, this suggests that peak blueshifted emission should occur near the maximum Doppler shift. Instead, the observed emission profiles tend to have peak emission intermediate between line center and the extreme wing.

One other possibility is that photons escape preferentially in the *lateral* direction. The motivation here is that in outflows, velocity gradients can lead to just such escape avenues. In this case, consider numerous discrete slabs distributed across a spherical shell. All else being equal, the brightest slabs will be those located near the plane of the sky owing to the lateral escape of radiation, and corresponding to frequencies around line center, which is more in accord with observations.

However, we caution that the Sobolev approximation applies when the Sobolev length l_{sob} is significantly smaller than the cooling length l_c (i.e., the extent of the hot gas region). A rough expression for a ratio of the two is

$$\frac{l_c}{l_{\text{sob}}} \approx \left(\frac{10^{10}}{n_e} \right) \left(\frac{v_{\text{sh}}}{v_{\text{th}}} \right) \left(\frac{R_{\odot}}{R_*} \right), \quad (6)$$

where n_e is in cm^{-3} and v_{sh} is the speed of the shocked gas in the observer’s frame. We will consider a spherically symmetric expanding wind with ambient number density

$$n_w(r) = \frac{\dot{M}}{4\pi \mu m_H r^2 v_r(r)}, \quad (7)$$

where \dot{M} is the mass-loss rate, v_r is the radial wind speed, and μ is the mean molecular weight per particle. The electron number density will naturally scale with the wind density. For typical hot stars, n_w ranges from 10^{10} – 10^{12} cm^{-3} at the wind base and drops to 10^7 – 10^9 by about $3R_*$, thereafter decreasing as r^{-2} . The Sobolev approximation

should thus be valid at most radii, except possibly in the densest regions of the inner wind acceleration where v_r is relatively small. But even at small radii, the Sobolev approach may be adequate if the shocked gas is of low density, as would be the case if the emission arises in reverse shocks. Alternatively, if $R_* \gg l_{\text{sob}} \gg l_c$, then there exist numerous pockets of hot gas within a Sobolev length. These would likely be optically thin, so treating them as statistically homogeneous allows us to recover the Sobolev approximation.

However, to say that the photons escape laterally implies that the lateral optical depth is less than the radial optical depth. So the effect of the velocity gradient carves the slab up into numerous radiatively independent and elongated “columns”. The short length of these columns is the Sobolev length, and the long length is the slab thickness. Given that the optical depth through the slab’s thickness was shown to be $\approx 10^2$, the columns can still be thick in the lateral direction for l_c/l_{sob} ranging from 10–100. This range is entirely reasonable given the preceding estimates, and so we next apply the Sobolev theory to deriving emission profile shapes to model the effects of lateral photon escape.

3. OPTICALLY THICK X-RAY EMISSION PROFILE SHAPES

3.1. Formalism for the Line Formation

For an envelope in bulk motion such that the flow speed greatly exceeds the thermal broadening, the locus of points contributing to the emission at any particular frequency in the line-profile is confined to an “isovelocity zone” (c.f., Mihalas 1978). These zones are determined by the Doppler-shift formula, namely

$$\nu_z = \nu_0 \left(1 - \frac{v_z}{c} \right), \quad (8)$$

where ν_z is the Doppler-shifted frequency and $v_z = -\mathbf{v}(\mathbf{r}) \cdot \hat{\mathbf{z}}$ is the projection of the flow speed onto the line of sight along z . The familiar Sobolev theory for line-profile calculation in moving media reduces the radiation transfer in the envelope to radiation

transfer within isovelocity zones (i.e., the transfer between different points in the envelope decouples if their relative velocity shift exceeds the local line broadening). Thus, the emergent line intensity along a given ray through the extended stellar envelope is given by

$$I_\nu = S_\nu(r) \left[1 - e^{-\tau_l(r,\mu)} \right] e^{-\tau_c(r,\mu)}, \quad (9)$$

where S_ν is the source function, τ_l is the Sobolev optical depth of the line where the ray intersects the isovelocity zone, and τ_c is the intervening absorptive optical depth.

Allowing for line emission from resonance line scattering and collisional de-excitation, and defining ϵ as the ratio of the collisional de-excitation rate (related to the rate of collisional excitation) to that of spontaneous decay, the source function is given by

$$S_\nu = \frac{\beta_c I_{\nu,*} + \epsilon B_\nu}{\beta + \epsilon(1 - \beta)}. \quad (10)$$

The two parameters β_c and β are respectively the penetration and escape probabilities, defined as

$$\beta_c = \frac{1}{4\pi} \int_{\Omega_*} \frac{1 - e^{-\tau_l}}{\tau_l} d\Omega, \quad (11)$$

and

$$\beta = \frac{1}{4\pi} \int_{4\pi} \frac{1 - e^{-\tau_l}}{\tau_l} d\Omega. \quad (12)$$

Adopting standard cylindrical coordinates (p, α, z) , with the observer at $+\infty$, the line optical depth is given by

$$\tau_l(p, z) = \int_z^\infty \sigma_l n_1 \delta(\nu - \nu_z) dz' = \frac{\sigma_l n_k(r) \lambda_0}{|dv_z/dz|_p}, \quad (13)$$

where σ_l is the frequency-integrated line cross-section, and the denominator on the right-hand side is the line-of-sight velocity gradient. In the case of a spherical flow, the line-of-sight velocity gradient is

$$\frac{dv_z}{dz} = \mu^2 \frac{dv}{dr} + (1 - \mu^2) \frac{v}{r}, \quad (14)$$

for $\mu = \cos \theta$ the direction cosine from the radial to the observer.

For the case of X-ray emission, we assume that the star is X-ray faint (i.e., no basal corona) such that $I_{\nu,*} = 0$ at X-ray energies. Also, the destruction probability ϵ depends on density, and so drops with radius. To make this explicit, we parameterize

$$\epsilon = \epsilon_0 \rho / \rho_0, \quad (15)$$

where ρ_0 and ϵ_0 are fiducial values with $\epsilon_0 \ll 1$ being typical. Under these conditions, the source function becomes

$$S_\nu \approx \frac{\epsilon}{\beta} B_\nu. \quad (16)$$

To compute the total emergent flux at a given Doppler shift in the line profile, we integrate over all intensity beams to obtain

$$F_\nu(v_z) = \frac{1}{D^2} \int_{v_z} I_\nu(p, z) p dp d\alpha, \quad (17)$$

where D is the distance from the Earth. Self-absorption by the hot plasma is ignored. The attenuation is therefore entirely from the cool wind component intervening between the observer and the point of emission. (For actual observations, one must also correct for the energy-dependent interstellar extinction, but we ignore its effects here since it does not alter the profile shape over the narrow extent of the line width.)

The wind optical depth is given by

$$\tau_c(p, z) = \int_z^\infty \kappa_c \rho_w(p, z) dz \quad (18)$$

with opacity κ_c and density ρ_w . The dominant opacity at the X-ray energies is photo-absorption by K-shell electrons. This opacity is calculated from

$$\kappa_c(E) = \frac{1}{\mu_N m_H} \sum_j \frac{n_j}{n_N} \sigma_j(E). \quad (19)$$

The opacity is a summation over cross-sections presented by different atomic species j and weighted by the relative abundance n_j/n_N , for n_N the number density of nuclei.

The line source function and a prescription for the wind attenuation are all the required pieces necessary to compute X-ray emission line profiles from stellar winds. The above expressions are applied in the next section for the specific case of a constant expansion flow.

3.2. The Constant Expansion Case

3.2.1. Justification of Assumption

The constant expansion wind is the most relevant case to consider for the problem at hand, since the continuum absorption by the winds of most O stars are expected to be optically thick over much of the X-ray band. The implication is that the observed X-rays emerge from the wind at depths of a few stellar radii or more. For the O star winds, the standard β -law velocity prescription for the radial distribution of wind speeds begins to asymptote around 1 to $1.5R_*$ above the wind base for the commonly used value of $\beta \approx 1$. Consequently for many lines, it is sufficient to model the emission profiles as if the entire wind were undergoing constant expansion. This case is also convenient because the expressions for the radiative transfer become analytic and provide interesting insight for better understanding the resulting profile shapes. However, there is at least one observational example of a line that seems to originate from deeper levels in the flow where the constant expansion assumption no longer applies (e.g., He-like S XV observed in ζ Pup by Cassinelli et al. 2001). In §5, we comment on the effect of the wind acceleration zone on the profile shape.

We begin by motivating the constant expansion assumption on more quantitative grounds. Owocki & Cohen (1999; for OB stars) and Ignace & Oskinova (1999; for WR stars) presented a scaling analysis for the X-ray emission from hot star winds based on an “exospheric” approximation. The observed X-ray emission (assumed to arise from an optically thin hot plasma) emerges only from radii exterior to the optical depth unity surface of radius r_1 , with X-rays at smaller radii assumed to be completely attenuated. The extent of this convenient scale r_1 derives from the photoabsorption by the wind along the line-of-sight. It is determined by the condition

that

$$\tau_c \approx 1 = \int_{r_1}^{\infty} \kappa_c \rho_w dr. \quad (20)$$

Assuming that $v(r) = v_\infty$ allows for an analytic evaluation of this integral, yielding

$$r_1(E) = \frac{\dot{M}}{4\pi v_\infty} \kappa_c(E). \quad (21)$$

This may seem circular, since we apply the constant expansion assumption here to justify that constant expansion should be adequate for the emission line calculation. But in fact, the integral of equation (20) minimizes the value of r_1 in the case of $v_r = v_\infty$, hence this is the conservative approach to showing that $r_1 \gtrsim 2R_*$ is valid over much of the X-ray band.

Using typical O star and wind parameters as in §2, a plot of r_1 versus wavelength is shown in Figure 1. The “jagged” features correspond to prominent photoabsorptive edges. Observed strong lines of H and He-like ions in stellar winds are generally located between 5 and 30 Å, as indicated at top. Note that 1 keV corresponds to about 12.4 Å (indicated by the vertical line in the plot), and so harder X-ray energies are at shorter λ , and vice versa. A horizontal line is provided where $r_1 = 2R_*$, beyond which the wind is essentially in constant expansion for O star winds. Many of the strong lines of interest occur at wavelengths for which $r_1 \gtrsim 2R_*$, where the approximation that $v_r \approx v_\infty$ will hold. A similar figure is provided by Cassinelli et al. (2001) in their discussion of *Chandra* observations of ζ Pup. They even tabulate r_1 values for several lines in their Table 2. It happens that ζ Pup has a slightly higher \dot{M} and lower v_∞ than we have used, so that even for Mg XII at 8.42 Å, Cassinelli et al. find $r_1 = 2.8R_*$.

3.2.2. Applying the Constant Expansion Assumption

Concluding that constant expansion is a reasonable assumption, we now consider again the line formation process under this condition. From equation (14), the line-of-sight velocity gradient reduces to

$$\tau_l = \frac{\sigma_l n_X(r) \lambda_0}{(v_\infty/r)(1-\mu^2)} \quad (22)$$

$$= T \left(\frac{R_*}{r} \right) (1-\mu^2)^{-1}, \quad (23)$$

where an optical depth scale T has been introduced. This scale is the “integrated optical depth” of the line along the line-of-sight (Groenewegen, Lamers, & Pauldrach 1989). The parameter T can be related to the column density of scatterers N_1 as follows,

$$N_1 = \int_R^\infty n_l dr \quad (24)$$

$$= \int_0^{v_\infty} \frac{\tau_l}{\sigma_l \lambda_0} dv_r. \quad (25)$$

Defining $T = \int_0^1 \tau_l dw$ for $w = v_r/v_\infty$, we obtain

$$T = \frac{\sigma_l \lambda_0}{v_\infty} N_1. \quad (26)$$

Unfortunately in the constant expansion approximation, the Sobolev optical depth of equation (23) contains a pole at $\mu = \pm 1$, corresponding to the extreme blue and red shifts. Physically of course, there is no real singularity problem. Because the wind is in constant expansion, there is no radial velocity gradient, hence the actual optical depth in the vicinity of $\mu = \pm 1$ is just $(v_\infty/v_{\text{th}})T$, for v_{th} the thermal broadening, because the radiative transfer corresponds to the case of a slab moving at constant speed v_∞ . Since $v_\infty/v_{\text{th}} \gtrsim 10$ can be expected, values of T exceeding a few will ensure that τ_l for $\mu \approx \pm 1$ will be large enough that the exponential factors in the Sobolev intensity of equation (9) and the escape probability of equation (12) are effectively zero, hence the “pole” problem will not be of significant concern. There are two subsequent implications for the constant expansion wind. (a) Instead of the line-of-sight integrated optical depth, T actually corresponds to τ_l at $\mu = 0$ and is thus a lateral optical depth scale. This is reasonable since for constant expansion, the line-of-sight velocity gradient arises only from the geometrical divergence of the spherical wind outflow. This scale is also the minimal Sobolev optical depth of $\tau_l(\mu)$ for any fixed r . (b) The

radial optical depth can be large, and so there is the possibility for effective photon trapping and substantial reabsorption by continuum opacity. This effect will be considered in §4.

Given that the thin line case has already been explicitly treated, we choose to focus on the thick line case. The major simplification that results comes in the escape probability. Recall that β varies between 0 and 1. For thin lines, β approaches the value of unity, meaning that photons scatter isotropically. For thick lines, β decreases to small values. Taking $\tau_l \gtrsim 1$, the escape probability reduces to

$$\beta \approx \frac{1}{2} \int_{-1}^{+1} \left(\frac{1}{T} \right) \left(\frac{r}{R_*} \right) (1-\mu^2) d\mu \quad (27)$$

$$= \frac{2}{3T} \left(\frac{r}{R_*} \right). \quad (28)$$

Clearly at large radius where τ_l drops below unity, the approximation breaks down. Defining $\gamma = 3TR_*/2r$, Figure 2 shows a plot of $\gamma \cdot \beta$, indicating that this product begins to plateau at unity around γ of 2. Since the constant expansion approximation applies only for r/R_* exceeding about 2–3, values of $T \gtrsim 10$ are required for lines to show interesting optical depth effects and for expression (28) to apply.

Continuing in the assumption that the line is optically thick, and noting that for constant expansion $\epsilon = \epsilon_0 (R_*/r)^2$, the source function reduces to the form

$$S_\nu(r) \approx \frac{3}{2} T \epsilon_0 B_\nu \left(\frac{R_*}{r} \right)^3. \quad (29)$$

The emergent intensity from a given point (r, μ) is given by

$$I_\nu \approx S_\nu(r) e^{-\tau_c(r, \mu)}, \quad (30)$$

where the continuum optical depth can be derived analytically (e.g., MacFarlane et al. 1991; Ignace 2001) as

$$\tau_c(r, \mu) = \tau_0 \left(\frac{R_*}{r} \right) \left(\frac{\theta}{\sin \theta} \right) \quad (31)$$

$$= \tau_0(E) \left(\frac{R_*}{r} \right) \frac{\cos^{-1} \mu}{\sqrt{1 - \mu^2}}, \quad (32)$$

for $\tau_0(E) = \kappa_c(E) \dot{M} / 4\pi R_* v_\infty$, the total continuum optical depth to the star along the line-of-sight.

To calculate the emission profile then requires an integration over the isovelocity zone corresponding to each frequency in the profile. For constant expansion, the isovelocity zones take the form of cones with $v_z = -v_\infty \mu$, so that constant v_z implies fixed μ . The integral to be evaluated is then

$$F_l(v_z) = \frac{2\pi}{D^2} \int_{r_{\min}}^{\infty} S_\nu(r) e^{-\tau_c(r, \mu)} r \sin^2 \theta dr, \quad (33)$$

where we have substituted for $p dp = \sin^2 \theta r dr$, and r_{\min} equals R_* for $v_z < 0$, but $R_*/\sin \theta$ for $v_z > 0$ owing to stellar occultation. An important point here is that the integral is over radius, so that the angular dependence is a constant of the integration.

With a change of variable $u = R_*/r$, the integral reduces to

$$\begin{aligned} F_l(v_z) &= \frac{2\pi R_*^2 \epsilon_0 B_\nu}{D^2} \left(\frac{3T}{2} \right) \sin^2 \theta \\ &\times \int_0^{u_{\max}} e^{-\tau_0 u \theta / \sin \theta} du. \quad (34) \\ &= \frac{3\pi R_*^2 \epsilon_0 B_\nu}{D^2} \\ &\times \left(\frac{T}{\tau_0} \right) \left(\frac{\sin^3 \theta}{\theta} \right) \left[1 - e^{-\tau_0 u_{\max} \theta / \sin \theta} \right] \end{aligned}$$

where $\theta = \cos^{-1}(-v_z/v_\infty)$, and $u_{\max} = 1$ for $v_z < 0$ and $u_{\max} = \sin \theta$ for $v_z > 0$. Figure 3 shows normalized emission profiles at various τ_0 . The case of $\tau_0 = 1$ indicates that the wind attenuation of X-rays is only mild, which invalidates our approximation that that X-rays emerge only where $v_r = v_\infty$; however, the $\tau_0 = 1$ case is included to demonstrate that the profile shape varies qualitatively little for a broad range of τ_0 values.

At large τ_0 , the line profile reduces to one of fixed shape described by

$$F_l(v_z) = \frac{3\pi R_*^2 \epsilon_0 B_\nu}{D^2} \left(\frac{T}{\tau_0} \right) \left(\frac{\sin^3 \theta}{\theta} \right), \quad (36)$$

which is to be contrasted against the analogous asymptotic limit for thin lines from Ignace (2001):

$$F_l(v_z) = \frac{2\pi j_0 R_*^3 \lambda_0}{D^2 v_\infty} \left(\frac{1}{\tau_0} \right) \left(\frac{\sin \theta}{\theta} \right). \quad (37)$$

The profile morphologies of the thin and thick asymptotic forms are compared in Figure 4. Note that both are asymmetric, with peak emission occurring at blueshifted velocities. However, the thick line is much more nearly symmetric in appearance, and its peak emission occurs not far from line center. In fact for the asymptotic limit of $F_l \propto \sin^3 \theta / \theta$, the location of the peak and the FWHM value of the profile can be easily computed. Peak emission occurs at $v_z = -0.24 \times v_\infty$, and the FWHM is $1.26 \times v_\infty$ (alternatively, the HWHM is $0.63 \times v_\infty$), which holds for *all* thick lines with $T \gtrsim$ a few. However, although resonance line scattering does conserve photon number, photons could be destroyed by other processes since there is a longer “dwell” time for photons than would be the case for optically thin lines that scatter only once. The next section considers the influence of reabsorption effects for the net line emission and profile shape.

4. OPACITY EFFECTS ON ABUNDANCE DETERMINATIONS

Optically thick resonance zones not only alter the profile shape, they also modify the fraction of X-ray line photons that are absorbed by the background continuum opacity prior to escape from the wind. They do this in two distinct ways. First, the preference for azimuthal emission slightly alters the average column depth through which the escaping flux must pass, and this changes the equivalent width of the line profiles. Second, if the Sobolev length l_{sob} is not negligible, as would be the case for lines that are highly broadened due to X-ray temperatures or microturbulence, then optically thick resonance zones can “trap” photons long enough to increase the total pathlength over which continuum absorption can occur (Hillier 1983). Both of these processes were calculated accurately by Hummer & Rybicki (1985). If these effects increase the reabsorption, then observed line equivalent widths will be reduced, and anomalously

low abundances might be inferred. Indeed, this is the interpretation given by Kitamoto et al. (2000) to the substantial shortfall in metal abundance inferred from optically thin fits to ASCA X-ray line observations of several OB stars. However, they did not apply the theory of Hummer & Rybicki (1985) in making their estimates, and here we show that they overestimated the degree to which photon destruction between scatterings in the line can reduce the observed line flux.

4.1. The Equivalent Width for Optically Thick Line Emission

To quantify the change in absorption due to the first effect above, note that optically thick lines in constant-expansion winds emit photons preferentially in directions azimuthal to the flow. Thus optically thick line photons emitted in generally outward directions (i.e., emitted toward the observer from the *near* side of the wind) will have an overall reduced chance of escape, since more of them are emitted from high impact parameters which experience greater continuum optical depth for a given radius. Conversely, the photons observed from the *far* hemisphere will be augmented on average, because then emitting more photons at higher impact parameters implies less occultation by the underlying wind. To ascertain which of these competing influences dominates, we write the expression for the ratio of the photon escape rate in the optically thick and thin limits, which also gives the equivalent-width (*EW*) ratio

$$\frac{EW_{\text{thick}}}{EW_{\text{thin}}} = \frac{\int_{R_*}^{\infty} dr r^2 \rho^2 \int_0^{\pi} d\theta 1.5 \sin^3 \theta e^{-\tau_0 R_* \theta / r \sin \theta}}{\int_{R_*}^{\infty} dr r^2 \rho^2 \int_0^{\pi} d\theta e^{-\tau_0 R_* \theta / r \sin \theta}} \quad (38)$$

In the above expression, equation (32) was used for the photoabsorptive optical depth, and the normalized emission profile from an optically thick resonance zone at constant expansion speed is $1.5 \sin^2 \theta$. It was also assumed that the line emissivity scales as ρ^2 , and that all line photons eventually escape their natal resonance region. Later we will consider the fraction that may be absorbed within the resonance zone.

Applying the condition $\rho \propto r^{-2}$ for constant expansion allows the elementary radial integrals in equation (38) to be carried out explicitly, giving in the limit of large total radial wind optical depth τ_0

$$\frac{EW_{\text{thick}}}{EW_{\text{thin}}} = 1.5 \left(\int_0^{\pi} d\theta \frac{\sin^4 \theta}{\theta} \right) \cdot \left(\int_0^{\pi} d\theta \frac{\sin^2 \theta}{\theta} \right)^{-1}. \quad (39)$$

When this expression is evaluated numerically, it is found that optically thick angular emission actually enhances escape, so the far-hemisphere effect dominates. This is the opposite sense as would be needed to help explain the abundance anomalies, but is of little significance because the magnitude of the increase in the equivalent width is only 2%.

4.2. Reduction in Line Equivalent Width By Continuum Reabsorption

The second effect mentioned above, reabsorption *within* the finite region in which the X-ray line photons are created and scattered, will certainly reduce the equivalent width when the lines become optically thick. This destruction mechanism is assumed to be dominated by continuum absorption, rather than thermalization within the line itself, and was considered by Kitamoto et al. (2000) to be a promising solution to low equivalent-width anomalies in ASCA observations of several OB winds. Unfortunately, they assume that photon escape from the X-ray-line resonance zone is diffusive, which produces an overly large total pathlength during which reabsorption can occur. Instead, escape of photons from the line-scattering region is known to occur by a “single-flight” escape process (Hummer & Rybicki 1982), whereby Doppler redistribution enables photons to rapidly reach the line wings. At that point the mean-free-path approaches the scale of the region and the escape is non-diffusive. In such a process, the total pathlength traversed scales linearly with the length scale for escape, not quadratically as assumed by Kitamoto et al. (2000).

Nevertheless, the total pathlength is indeed enhanced by optically thick line scattering, so some of the abundance anomaly may be explained by

this process. The basic theory of how continuum opacity affects line formation in the Sobolev approximation was developed by Hummer & Rybicki (1985), so only a rough sketch of their derivation is included here, expressed in intuitively motivated probabilistic terms. For a two-level atom in complete frequency redistribution, common assumptions for line formation in the Sobolev approximation, the line source function may be written

$$S_l = \frac{\varepsilon B}{(\varepsilon + \xi)}, \quad (40)$$

where ε is the destruction probability per scattering and is assumed to be small, B is the Planck function, and ξ gives the fraction of radiative downward transitions in the atom that are not balanced locally by radiative upward transitions. Since εB here describes the photon creation rate, and it is likely that $\varepsilon \ll \xi$, the essential statement for our purposes is that $S_l \propto \xi^{-1}$, due to multiple scattering within the optically thick resonance layer. Hence ξ^{-1} may be associated with the expected number of scatterings each photon undergoes between creation and escape.

In the first-order escape probability approximation, which is especially applicable in the spirit of the Sobolev approximation, ξ is replaced by the probability that a line photon which has just been emitted will *not* be scattered again in the line. If the only other possibility is escape, then in the notation above this implies $\xi \cong \beta$. However, the presence of continuum opacity allows for another alternative to scattering, which is absorption within the resonance zone. Thus ξ is increased, and S_l reduced, by the presence of continuum absorption (e.g., Puls & Hummer 1988).

The expression for the probability that no line scattering will occur is most easily found by first writing the probability that a line scattering *will* occur. This is pieced together by first noting that the photon is assumed to be emitted isotropically, so is emitted randomly in a flat distribution over direction cosine μ . In complete redistribution, it will also be emitted randomly over the frequency profile $\phi(x)$, typically a Doppler profile. Given an emission within $d\mu$ of angle μ and within dx of frequency x , in the Sobolev approximation in an expanding wind, the photon propagates effectively not in real space

but rather toward redder comoving frequencies x' .

If the photon makes it to some x' along direction μ , the probability of scattering within dx' of x' is given simply by $\tau_\mu \phi(x') dx'$, where τ_μ is the Sobolev optical depth of the resonance zone along direction μ . In the absence of continuum opacity, the probability that the photon will make it to x' is thus given by

$$P(x, x', \mu) = e^{-\tau_\mu [\Phi(x) - \Phi(x')]}, \quad (41)$$

where

$$\Phi(x) - \Phi(x') = \int_{x'}^x dy \phi(y), \quad (42)$$

and it is canonical to set $\Phi(-\infty) = 0$ via the definition

$$\Phi(x) = \int_{-\infty}^x dy \phi(y). \quad (43)$$

In all, one obtains

$$\xi \cong \beta = 1 - \frac{1}{2} \int_{-1}^1 d\mu \int_{-\infty}^{\infty} dx \phi(x) \int_{-\infty}^x dx' \tau_\mu P(x, x', \mu). \quad (44)$$

Here τ_μ and β are given in equations (22) and (27) respectively, and if we denote the azimuthal Sobolev line optical depth as

$$\tau_l = T \frac{R_*}{r}, \quad (45)$$

then equation (44) yields, in agreement with equation (27),

$$\xi \cong \frac{2}{3\tau_l}. \quad (46)$$

The introduction of continuum opacity simply reduces $P(x, x', \mu)$ by an additional factor which represents the probability of continuum absorption during propagation from x to x' . If the effective line optical depth over the interval dx' is $dx' \tau_\mu \phi(x')$, then the continuum optical depth over that propagation interval is $dx' \tau_\mu C$, where

$$C = \frac{\kappa_c}{\kappa_l} \quad (47)$$

and κ_c and κ_l are respectively the continuum and mean line opacities. By its definition, the continuum-absorption parameter C is readily shown to be related to the ratio of τ_c , the radial continuum optical depth to the resonance zone in question, and τ_l , the azimuthal Sobolev optical depth of that resonance zone, via

$$C = \left(\frac{\tau_0}{T}\right) \left(\frac{v_{\text{th}}}{v_\infty}\right) = \left(\frac{\tau_c}{\tau_l}\right) \left(\frac{v_{\text{th}}}{v_\infty}\right) \quad (48)$$

in a steady spherical wind at constant speed.

Note once again that here v_{th} represents all of the velocity broadening over the Sobolev length, and so may include more than the thermal speed of the ion in question and may approach the hydrodynamical sound speed of the hot gas, which is at the level of tens of percent of the terminal speed. If v_{th} is much greater than about 1/10 of v_∞ , the Sobolev approximation itself may come into question, so this may be viewed as a rough upper bound for the broadening to which our theory can apply. Nevertheless, since $\tau_c \sim 1$ where the observable line emission forms, and $\tau_l \gtrsim 10$ is required to apply optically thick line theory, the condition $v_{\text{th}} \lesssim v_\infty/10$ implies that $C \lesssim 10^{-2}$. This unusually large upper bound for the continuum opacity, relative to the lines, is a manifestation of an implicit assumption that the hot line-forming gas represents only a small fraction of a wind dominated by cooler and continuously-absorbing gas.

By integrating the continuum optical depth encountered by a photon propagating from x to x' , the absorption-modified expression for $P(x, x', \mu)$ then becomes

$$P(x, x', \mu, C) = e^{-\tau_l[\Phi(x) - \Phi(x')]} \times e^{-\tau_l C(x - x')}, \quad (49)$$

and so when ξ is approximated by the new probability that a scattering does *not* occur, the result is

$$\begin{aligned} \Delta\xi(C) &= 1 - \frac{1}{2} \int_{-1}^1 d\mu \int_{-\infty}^{\infty} dx \phi(x) \\ &\quad \times \int_{-\infty}^x dx' \phi(x') \tau_\mu P(x, x', \mu, C) \end{aligned} \quad (50)$$

This can be written

$$\xi(C) = \xi(0) + \Delta\xi(C) \quad (51)$$

where

$$\xi(0) = \beta = \frac{2}{3\tau_l} \quad (52)$$

and

$$\begin{aligned} \Delta\xi(C) &= \int_0^1 d\mu \int_{-\infty}^{\infty} dx \phi(x) \\ &\quad \times \int_{-\infty}^x dx' \phi(x') \tau_\mu P(x, x', \mu, C) \end{aligned} \quad (53)$$

was derived in an alternate notation by Hummer & Rybicki (1985).

The correction to ξ is found to become significant when $C\tau_l \sim 0.1$, and when this is true, continuum reabsorption within the line approaches the static limit for an infinite atmosphere. Then the tabulated results of Hummer (1968) show that a reasonable approximation for $\Delta\xi(C)$ when C is within an order of magnitude of 10^{-2} is

$$\Delta\xi(C) \cong 4C. \quad (54)$$

This implies that the factor by which the line source function S_l must be reduced to account for continuum absorption when $C\tau_l \sim 0.1$ is

$$\frac{S_l(C)}{S_l(0)} \cong \frac{\xi(0)}{\xi(C)} \cong \frac{\beta}{(\beta + \Delta\xi(C))} \cong \frac{1}{(1 + 6C\tau_l)}. \quad (55)$$

As mentioned above, $C\tau_l \sim v_{\text{th}}/v_\infty$ near the X-ray photosphere, so when v_∞ is of order 10^3 km s^{-1} , $C\tau_l$ can reach values as large as 0.1 only when the line broadening represents a substantial fraction of the sound speed in the X-ray gas. Interestingly, although the parameter C does affect the source-function correction at any given radius, it is not directly relevant to the integrated equivalent width, because increasing κ_c simply moves the resonance zones of interest out to larger radii and therefore lower density. This regulates the reabsorption within the resonance zone in a manner that is independent of C . Instead, it is the parameter v_{th}/v_∞ which controls the correction to the equivalent width, so we give this parameter its own designation, u_{th} , and note that $C\tau_l = u_{\text{th}}\tau_c$. The equivalent width correction is calculated by inserting $S_l(C)/S_l(0) = (1 + \Delta\xi/\beta)^{-1}$ from equation (55) into the integral in the numerator of equation (38), and the result is shown in Figure 5.

It is apparent from this figure that the equivalent-width correction is only substantial when u_{th} is appreciably elevated beyond the purely thermal motions of the heavy ions. This might occur, for example, if overpressures at the sonic scale in the hot gas were to accelerate flows stochastically on the scale of the Sobolev length, which would yield superthermal microturbulence in the X-ray lines. In such a scenario, Figure 5 shows that the observed equivalent widths could be reduced by up to about

40% before the basic assumptions of this model are severely violated. Such a substantial reduction could certainly alter the inferred abundance of the ion involved, although perhaps not to the degree expected by Kitamoto et al. (2000). Whether or not it could provide a complete explanation for the observed abundance anomalies remains a question for more detailed physical models; the sole conclusion here is that if abundance anomalies are to be explained by continuum absorption within the line resonance zones, some type of microturbulent broadening is required to generate Sobolev lengths with $l_{\text{sob}} \gtrsim 0.1r$, straining the Sobolev approximation itself. This possibility is not beyond reason, however, as a radial variant on this same concept has already been invoked (Lucy 1982) to explain “black troughs” in UV resonance-line spectra of OB winds (Lamers & Morton 1976; Prinja, Barlow, & Howarth 1990).

4.3. The Influence of Continuum Absorption on Line Profile Shape

Appreciable values of $C\tau_l$ not only effect the equivalent width in low-resolution spectra, they also alter the profile shape at high resolution. Since $\tau_c = \tau_0(R_*/r)$ implies that $C\tau_l \propto r^{-1}$, the effect of continuum absorption on the line becomes less important at large radii. Thus when the factor given by equation (55) is inserted into equation (33), the profile shape is altered by the fact that S_l will now fall less rapidly than the r^{-3} of equation (29). Since C is fairly small, this will only be important when τ_l is large, and in that limit the modified equation (34) becomes

$$F_l(v_z) = \frac{3\pi R_*^2 \epsilon_0 B_\nu}{D^2} \left(\frac{T}{\tau_0}\right) \left(\frac{\sin^3 \theta}{\theta}\right) f\left(\frac{1}{6} \frac{v_\infty}{v_{\text{th}}} \frac{\theta}{\sin \theta}\right), \quad (56)$$

where we have defined

$$f(x) = x e^x \int_x^\infty dy \frac{e^{-y}}{y}. \quad (57)$$

This profile shape is plotted in Figure 6 for a range in values of v_{th}/v_∞ . Note that if $v_{\text{th}} \ll v_\infty$, f approaches unity and we recover the $\tau_0 \gg 1$ limit of equation (34). The unphysical limit $v_{\text{th}} \gg v_\infty$ can

be used as a check, since then $f(x)$ is of order x , and the profile approximates the (symmetric) parabolic shape $1 - v_z^2/v_\infty^2$ characteristic of μ -dependent line emissivity over a “skin depth” of fixed continuum mean-free-path. This limit is of course unphysical because it completely violates the approximations made, particularly the Sobolev approximation. Instead, the importance of the profile shapes seen in Figure 6 applies for much more modest values of v_{th}/v_∞ , which are seen to reduce the profile asymmetry even further than that due solely to continuum reabsorption *outside* the resonance zone.

5. SUMMARY AND DISCUSSION

Our paper considers the role of optical depth in X-ray emission-line formation in stellar winds. The line photons are assumed to be created by collisional processes, and thus scale with the square of the density, and may then be resonantly scattered. We have demonstrated that strong lines with sufficient opacity to multiply scatter emerging photons will alter the observed profile shape in a recognizably characteristic way. Our line synthesis has taken into account the “cool” wind photoabsorption, which can strongly attenuate X-ray photons at soft and intermediate energies.

We argue that when the wind is highly optically thick to photoabsorption, it is adequate to consider constant expansion for the purpose of computing the line profile. In this limit the expressions for the radiative transfer can be solved analytically. Lines that are optically thick over a resonance zone are found to have profile shapes that scale as $F_l \propto \sin^3 \theta/\theta$, which is to be compared to the analogous thin-line case of $\sin \theta/\theta$, where the observed velocity shift is $v_z = -v_\infty \cos \theta$.

It useful to compare these theoretical values against those measured for ζ Pup by Cassinelli et al. (2001). These authors list the HWHM and centroid shift of five lines in their Table 2 (we ignore the N VII profile which is clearly different owing to its flat-topped morphology). The centroid shifts range between -460 and -700 km s $^{-1}$, and the HWHMs range from 970 to 1340 km s $^{-1}$. Cassinelli et al. quote a terminal speed of 2250 km s $^{-1}$. Hence peak line emissions fall between -0.2 and -0.3 of v_∞ , and

the HWHM are around 0.4 to 0.6 of v_∞ . This data is compared with the asymptotic thick line predictions in Figure 7 (i.e., without reabsorption effects). The HWHMs all fall below our predicted value, but the centroid values are all consistent with our thick line results. This is somewhat surprising in light of our rather simplified assumptions and the fact that we do not allow for any radial variation of the hot gas temperature. We must interject the caution that we have not actually tried to *fit* the observed profiles, only compare global characterizations in the form of where peak emission occurs and the overall line width. More detailed line fitting to the data is necessary to determine categorically whether thin or thick lines better represent each observation, but our simple comparison suggests that optical-depth effects could be a key element to interpreting the observations, and that the ζ Pup data is more consistent with the standard wind-shock paradigm than previously thought.

However for ζ Ori, θ^1 Ori C, and δ Ori, the observed emission profiles are shown or claimed to be extremely symmetric, with little or no centroid shift. (Note that for observed line profiles of modest S/N and spectral resolution, our theoretical line shapes could match the symmetric appearance only if the central line wavelengths were misplaced slightly to the blue.) Thick resonance-line scattering by itself is not able to explain such symmetries, at least not without allowing parameters such as T_X to vary with radius, or introducing new free parameters. However, a consideration of reabsorption by the continuum opacity within a highly optically thick resonance zone can in principle lead to symmetric lines with an inverted parabolic shape in the limiting case, and suppression of the line emission. The effect depends on the relative line broadening v_{th}/v_∞ , leading to a modest effect for only thermal broadening by the hot gas, but can significantly reduce the line equivalent width ($\approx 40\%$) if there are extreme microturbulent motions of order $0.25v_\infty$. For this latter case, the influence of reabsorption by thick resonance-line scattering may help to understand both the line symmetry in these three stars and the sub-solar abundance problem. One major difficulty is whether observed lines have sufficiently high values of T so that our results apply. A second is, where are the optically thin lines that do show the theoretically expected morphology for distributed wind shocks,

and do such lines also exhibit abundance problems?

One effect that we have ignored has been the influence of the wind acceleration zone. In lower-density winds, the formation of lines at intermediate X-ray energies will sample these inner radial depths of the wind. This will lead to a source function of the form $S_\nu \propto (\rho_w/\beta) = \tau_l/(r^2v_r)$, where v_r varies rapidly in the span of just $1-2R_*$ and τ_l depends on the velocity gradient. However, the wind attenuation will also be enhanced, plus reabsorption effects of line photons will be more severe. So there are strongly competing effects between shifting the profile to greater symmetry versus asymmetry, and a more detailed analysis will be required in general.

Another effect that has been ignored is the influence of “porosity”. We have treated the hot X-ray emitting gas as being thoroughly mixed throughout the ambient wind flow. However, the wind is probably highly structured in density and velocity, both radially and laterally. If the porosity is severe, in the sense that cool absorbing wind material is strongly clumped such that the mean-free-path for X-ray photons becomes quite long, then this may explain the lack of profile symmetry in ζ Ori, θ^1 Ori C, and δ Ori (Cassinelli 2001, private communication). Of course, one must then pose the question of why ζ Pup is different.

Finally, should optical-depth effects be relevant for other early-type stars? The B star winds are far less dense than O stars, so that except at the softest energies, the X-rays from the entire wind probably emerge free of attenuation. In this case, the line synthesis presented by Owocki & Cohen (2001) will likely be able to match the profiles, should they be observed. On the other hand, the Wolf-Rayet winds are substantially denser than for the O stars, so dense that r_1 is 10’s and even 100’s of R_* in extent. In this case, strong lines are probably optically thick over much of the wind, but this is compensated by the fact that the observed line emission emerges from large radius. Such lines can certainly be assumed to form in a constant-expansion wind, so if thin, the asymptotic profile shape derived by Ignace (2001) should apply, and if thick, the asymptotic profile shape derived here applies instead. These conclusions need to be tested by future observations.

We express appreciation to Joe Cassinelli, Stan Owocki, John Hillier, and David Cohen for comments in relation to the possibility of thick X-ray lines. We also gratefully acknowledge the referee, John Castor, for several insightful and helpful remarks. This research was supported by NASA grant NAG5-9964.

REFERENCES

- Berghöfer, T. W., & Schmitt, J. H. M. M. 1995, *Adv. Space Res.*, 16, 163
- Berghöfer, T. W., Schmitt, J. H. M. M., Danner, R., & Cassinelli, J. P. 1997, *A&A*, 322, 167
- Cassinelli, J. P., & Olson, G. L. 1979, *ApJ*, 229, 304
- Cassinelli, J. P., Miller, N. A., Waldron, W. L., MacFarlane, J. J., & Cohen, D. H. 2001, *ApJ*, 554, L55
- Castor, J. I., Abbott, D. C., & Klein, R. I. 1975, *ApJ*, 195, 157
- Feldmeier, A., Puls, J., & Pauldrach, A. W. A. 1997, *A&A*, 322, 878
- Friend, D. B., & Abbott, D. C. 1986, *ApJ*, 311, 701
- Groenewegen, M. A. T., Lamers, H. J. G. L. M., & Pauldrach, A. W. A. 1989, *A&A*, 221, 78
- Harnden, F. R., Jr., Branduardi, G., Gorenstein, P., Grindlay, J., Rosner, R., Topka, K., et al. 1979, *ApJ*, 234, L51
- Hillier, D. J. 1983, Ph.D. thesis, Australian National University
- Hillier, D. J., Kudritzki, R. P., Pauldrach, A. W., Baade, D., Cassinelli, J. P., Puls, J., & Schmitt, J. H. M. M. 1993, *A&A*, 276, 117
- Hummer, D. G., 1968, *MNRAS*, 138, 73
- Hummer, D. G., & Rybicki, G. B. 1982, *ApJ*, 254, 767
- Hummer, D. G., & Rybicki, G. B. 1985, *ApJ*, 293, 258
- Ignace, R., & Oskinova, L. M. 1999, *A&A*, 348, L45
- Ignace, R. 2001, *ApJ*, 549, L125
- Kahn, S. M., Leutenegger, M., Cottam, J., Rauw, G., Vreux, J. M., den Boggende, T., Mewe, R., & Guedel, M. 2000, *A&A*, 365, L312
- Kitamoto, S., & Mukai, K. 1996, *PASJ*, 48, 813
- Kitamoto, S., Tanaka, S., Suzuki, T., Torii, K., Corcoran, M. F., & Waldron, W. 2000, *AdSpR*, 25, 527
- Kudritzki, R. P., Palsa, R., Feldmeier, A., Puls, J., & Pauldrach, A. W. A. 1996, in *MPE Report 263, Röntgenstrahlung from the Universe*, ed. H. U. Zimmerman, J. Trümper, & H. Yorke, 9
- Lamers, H. J. G. L. M. & Morton, D. C. 1976, *ApJS*, 32, 715
- Lucy, L. B. 1982, *ApJ*, 255, 286
- Lucy, L. B., & Solomon, P. M. 1970, *ApJ*, 159, 879
- Lucy, L. B. & White, R. L. 1980, *ApJ*, 241, 300
- MacFarlane, J. J., Cassinelli, J. P., Welsh, B. Y., Vedder, P. W., Vallergera, J. V., & Waldron, W. L. 1991, *ApJ*, 380, 564
- Mihalas, D. 1978, *Stellar Atmospheres*, (San Francisco: Freeman)
- Miller, N. A., Cassinelli, J. P., Waldron, W. L., MacFarlane, J. J., & Cohen D. H. 2001, *ApJ*, submitted
- Oskinova, L. M., Ignace, R., Brown, J. C., & Cassinelli, J. P. 2001, *A&A*, 373, 1009
- Owocki, S. P., Castor, J. I., & Rybicki, G. B. 1988, *ApJ*, 335, 914
- Owocki, S. P., & Cohen, D. H. 1999, *ApJ*, 520, 833
- Owocki, S. P., & Cohen, D. H. 2001, *ApJ*, 559, 1108
- Pauldrach, A., Puls, J., & Kudritzki, R. P. 1986, *A&A*, 164, 86
- Pollock, A. M. T. 1987, *ApJ*, 320, 283
- Pollock, A. M. T., Haberl, F., & Corcoran, M. F. 1995, in *IAU Symp. #163, Wolf-Rayet Stars: Binaries, Colliding Winds, Evolution*, ed. K. A. van der Hucht, P. M. Williams, (Kluwer: Dordrecht), 191
- Prinja, R. K., Barlowe, M. J., & Howarth, I. D. 1990, *ApJ*, 361, 607
- Puls, J. & Hummer, D. G. 1988, *A&A*, 191, 87
- Raymond, J. C., & Smith, B. W. 1977, *ApJS*, 35, 419
- Schulz, N. S., Canizares, C. R., Huenemoerder, D., & Lee, J. C. 2001, *ApJ*, 545, L135
- Seward, F. D., & Chlebowski, T. 1982, *ApJ*, 256, 530

Seward, F. D., Forman, W. R., Giacconi, R.,
 Griffiths, R. E., Harnden, F. R., Jr., Jones,
 C., & Pye, J. P. 1979, ApJ, 234, L55
 Sutherland, R. S., & Dopita, M. A. 1993, ApJS, 88,
 253
 Waldron, W. L. 1984, ApJ, 282, 256
 Waldron, W. L., & Cassinelli, J. P. 2001, ApJ, 548,
 L45

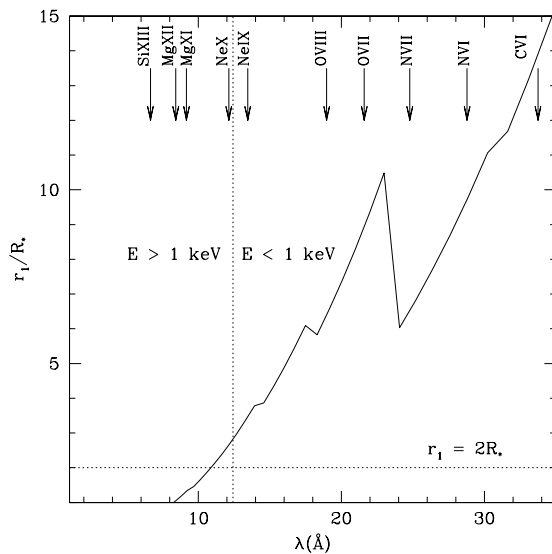


Fig. 1.— A plot of the optical depth unity radius from the wind photoabsorptive opacity versus wavelength in the X-ray band. Typical O star and wind parameters are assumed. The horizontal dotted line indicates $r_1 = R_*$, and the vertical line gives the location of $E = 1$ keV, corresponding to $\lambda = 12.4\text{\AA}$. The location of strong emission lines are noted.

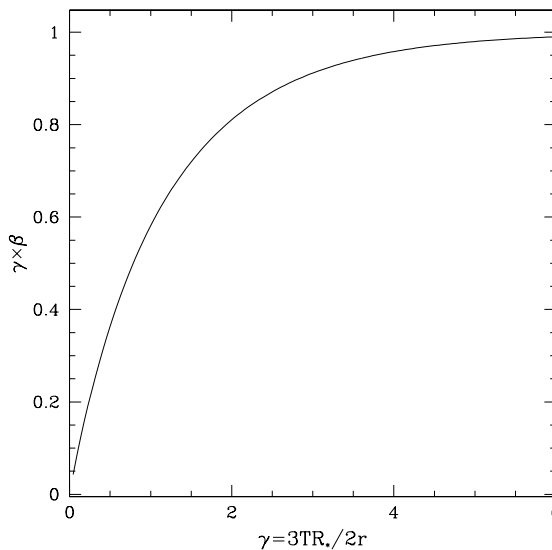


Fig. 2.— A plot of how rapidly the line escape probability approaches the asymptotic limit of $\beta = \gamma^{-1} = 2r/3TR_*$. The vertical is shown as the product $\gamma\beta$. Clearly β is nearing its asymptotic form at $\gamma \approx 2$.

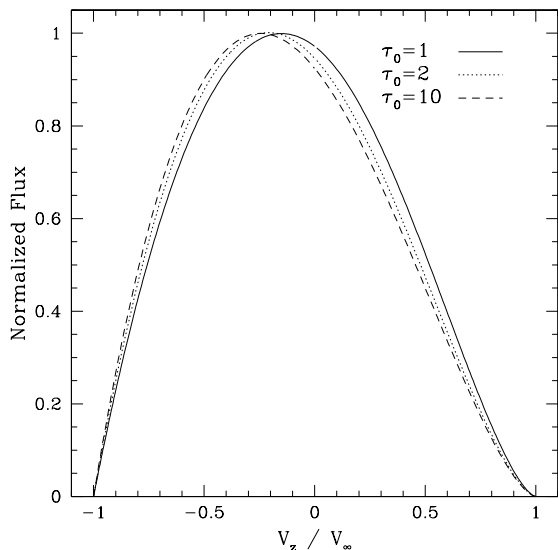


Fig. 3.— A comparison of normalized thick line profiles showing the influence of the wind attenuation with $\tau_0 = 1, 2,$ and 10 as indicated. As long as the line is optically thick in resonance line scattering, the width and centroid shift of the line peak are not strongly affected by the wind photoabsorption.

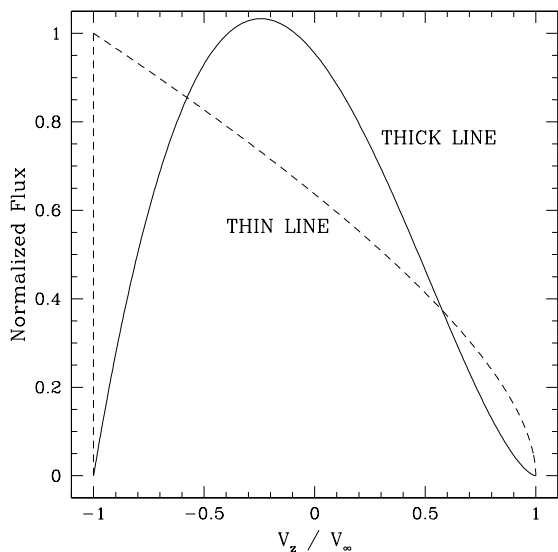


Fig. 4.— A comparison of thin versus thick X-ray emission lines, both in the asymptotic regime of large τ_0 . Both lines are asymmetric with a blueshifted centroid of the emission peak, but the thick line is more symmetric than is the thin case.

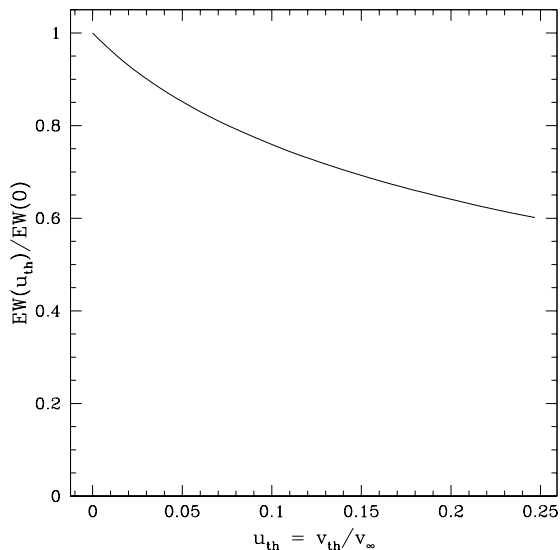


Fig. 5.— A plot of how the equivalent width (EW) of thick lines are reduced as a function of the degree of continuum reabsorption as parametrized by the line broadening $u_{\text{th}} = v_{\text{th}}/v_{\infty}$. The normalization $EW(0)$ corresponds to the line equivalent width with $u_{\text{th}} = 0$. In the presence of microturbulence, values of u_{th} may rise to a couple of tenths leading to a modest reduction (20–40%) in the line EW .

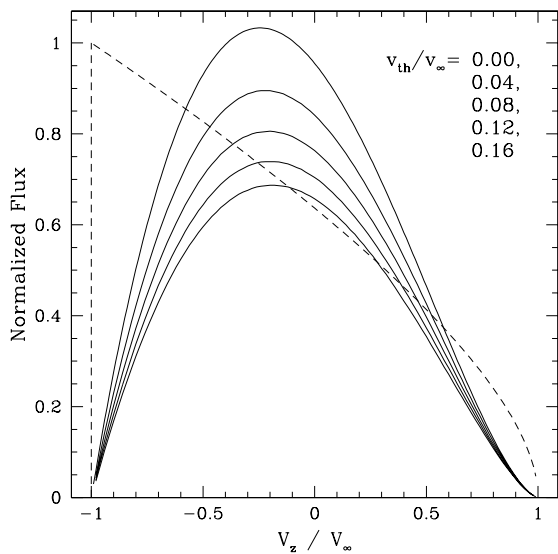


Fig. 6.— A plot of different thick line profiles as v_{th}/v_{∞} is increased from 0 to 0.16 (solid lines), with a thin line profile shown for comparison (dashed). The influence of reabsorption is twofold: larger values of the broadening diminish the overall amount of line emission, and the profile becomes more symmetric in shape. In the unphysical limit of $v_{\text{th}}/v_{\infty} \gg 1$, the profile will take on the purely symmetric form of $(1 - v_z^2/v_{\infty}^2)$.

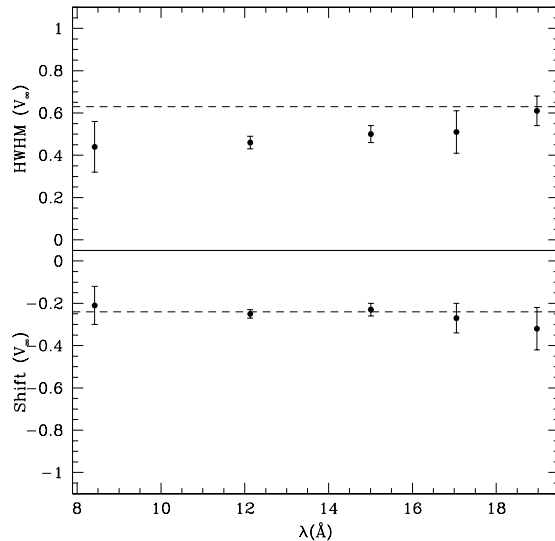


Fig. 7.— A comparison of the HWHM and centroid shift (both normalized by v_{∞}) for ζ Pup observed with *Chandra* versus the predictions of our limiting thick line case. The points correspond to five different lines with errorbars as tabulated in Cassinelli et al. (2001). Although the HWHMs are slightly smaller than predicted, the centroid values agree well with our theoretical results. Curiously, lines at longer wavelength appear more nearly consistent with our predicted result. At the longer wavelengths, the line emission escapes from larger radius (see Fig. 1) where the constant expansion approximation that we have used is best satisfied.